Crystallization Behavior of Polypropylene/Ethylene Butene Copolymer Blends

Jinhai Yang,[1] James L. White[2]

[1]*Department of Polymer Science and High Performance Materials, University of Southern Mississippi, Hattiesburg, Mississippi*
[2]*Department of Polymer Engineering, The University of Akron, Akron, Ohio*

Received 28 December 2009; accepted 21 August 2010
DOI 10.1002/app.35184
Published online in Wiley Online Library (wileyonlinelibrary.com).

ABSTRACT: One polypropylene (PP) was mixed with two ethylene butene copolymers (EBM). EBM1 had 12.5 mol % of butene and was immiscible with the PP. EBM2 had 51.6 mol % of butene and was miscible with the PP. The dispersed PP in EBM1 showed fractionalized crystallization behavior with a crystallization temperature at around 45°C and a much slower isothermal crystallization rate comparing to the neat PP. The PP did not exhibit fractionalized crystallization behavior in EBM2. EBM1 did not decrease both the crystallization and melting temperatures of the continuous PP. However, EBM2 could decrease both the two temperatures. It was found that EBM2 could largely suppress the epitaxial lamellar branching of the PP.
 J Appl Polym Sci 000: 000–000, 2012

Key words: polypropylene; ethylene butene copolymer; blends; miscibility; fractionalized crystallization; epitaxial lamellae

INTRODUCTION

Isotactic polypropylene (iPP) is a very important polymer material for both industry and academy. It was the first synthesized polymer with controlled stereospecific structure with Ziegler-Natta catalyst in 1954.[1–2] In industries, it is widely used from elastomers compounded with rubbers to high modulus composites compounded with glass fibers. It also exhibits many interesting crystallization behaviors. It could form both positive and negative spherulites dependent on crystallization temperatures.[3] It was extensively reported to exhibit double melting peaks dependent on crystallization temperatures.[4–13] The isothermal crystallization temperatures can be divided into four regions: below 122°C (region I); from 122 to 133°C (region II); from 133 to 152°C (region III); above 152°C (region IV). When crystallizing in region II/IV, it showed one melting peak. When crystallizing in region I/III, it showed double melting peaks. The double melting peaks formed in region I were because of the recrystallization and could be eliminated by high DSC heating rate (usually above 40°C/min).[5,10,11] The double melting peaks formed in region III were from two groups of lamellae and could not be eliminated by fast DSC heating scanning.[9–13] These two groups of lamellae originated from the unique epitaxial crystallization behavior of iPP. It was first reported from solution crystallized iPP[14,15] and existed extensively in melt crystallized iPP.[16–21] These structures are composed of two parallel sets of lath-like chain folded lamellae crossing each other at an angle of about 100 (or 80) degree.[16,22]

The crystallization behavior of PP in its blends with other polymers was also widely studied. It demonstrated a fractionated crystallization behavior[23–26] when it was dispersed in a matrix whose crystallization temperature was lower than PP's. Fractionated crystallization is one phenomenon: when one polymer is dispersed into another polymer as dispersed phase its crystallization temperature can be decreased largely. It is a general crystallization behavior of blend systems and was reported in metal blends and various polymer blends.[27–30]

The miscibility between polypropylene and ethylene α-olefin copolymers was also studied and found dependent on the α-olefin contents. It was reported that when butene or hexene contents were more than around 50 mol % their ethylene copolymers were miscible with iPP.[31–34] It was reported that the miscible ethylene butene copolymer could obviously decrease the spherulite growth rate of iPP, but the immiscible ethylene butene copolymer had no effect on the spherulite growth rate.[33]

It is our purpose to compare the crystallization behavior of iPP in its miscible and immiscible blends with two ethylene butene copolymers at a broad composition range, at isothermal, nonisothermal, and melt spinning crystallization processes.

Correspondence to: J. Yang (shinnningsea@gmail.com).

EXPERIMENTAL

Materials

One polypropylene (PP) was used. It had a density of 0.9 g/cm^3, M_w of 409,000, and M_n of 58,400. Two ethylene butene copolymers (EBM) were used. EBM1 was provided by Exxonmobil Chemical Co. and its trade name was Exact 4041. It had 12.5 mol % of butene, a density of 0.878 g/cm^3, M_w of 95,000, and M_n of 38,000. EBM2 was provided by Tosoh Corp. It had 57.4 mol % of butene, M_w of 270,000, and M_n of 130,000. The two EBMs exhibited different miscibility with the PP because of their different butene contents.

Blend preparation

PP/EBM1 blends were mixed in a CW Brabender laboratory mixer; 65 g of blend pellets were mixed in the chamber at 190°C at 80 rpm for 10 min. The blend melts were then cooled down to room temperature in 5 min in a cool plate compression molding machine. PP/EBM2 blends were prepared in a Haake twin screw micro-compounder because of its limited amount. To avoid its degradation in mixing, it was first mixed with thermal stabilizers; 70 g of EBM2 together with 140 mg Irganox 1010 and 140 mg Irganox 1076 (from Ciba) was mixed in a CW Brabender laboratory mixer at room temperature at 80 rpm for 6 min. It was stored in a desiccator; 5 g of PP/EBM2 blends was loaded in a Haake twin screw micro-compounder and mixed at 190°C and at 200 rpm for 5 min. The blends were named as PPEBM1-X or PPEBM2-X, where X was the percentage number of the PP content in the blends.

Scanning electron microscopy (SEM)

The blends were cut in liquid nitrogen to make fresh surface. EBM phase was etched away in heptane at 90°C for 1 h. The samples were dried in a vacuum oven at 40°C for 1 h and then coated with silver and observed in a SEM (Hitachi *S*-2150).

Dynamic mechanical analysis (DMA)

The glass transition temperatures of the blends were measured by dynamic mechanical analysis (DMA) (Pyris Diamond) with a tension mode. The heating rate was 4°C/min and the frequency was 10 Hz. The samples were compression molded at 190°C for 10 min. The samples had a thickness of 0.3 mm, a width of 10 mm, and a gauge of 20 mm.

Differential scanning calorimetry (DSC)

The melting and crystallization of both pure polymers and their blends were measured in a Perkin–Elmer DSC-7 with a 20 cm^3/min nitrogen gas flow. The sample weight was between 5 and 8 mg. Samples were first heated to 230°C at 40°C/min and held there for 5 min, then cooled down to −30°C at 20°C/min, then heated to 230°C at 20°C/min. The melting temperatures were decided from the second heating cycle. The crystallization temperatures were decided from the cooling cycle.

The isothermal crystallization behavior was tested. The samples were first heated to 230°C at 40°C/min and held there for 5 min, and were then cooled down to 120°C at 80°C/min. The isothermal crystallization behaviors were analyzed based on Avrami[35] theory as

$$X_c = 1 - \exp(-kt^n) \tag{1a}$$

$$\ln[-\ln[1 - X_c]] = \ln k + n \ln t \tag{1b}$$

where t is crystallization time, X_c is relative crystallinity defined as the ratio of the crystallinity at time t to the crystallinity when the crystallization is finished, k is a crystallization rate constant, and n is nucleation parameter.

Melt spinning

The blends were melt spun using an Instron Capillary rheometer at 190°C. The capillary die had a diameter of 1.59 mm, length-diameter ratio (L/D) of 28.5, and entrance angle of 90°. The extrusion rate was 0.054 cm^3/min giving an apparent shear rate of 2.4/s.

WAXD

Wide angle X-ray diffraction (WAXD) was used to investigate the crystal structure of the PP and its blends fibers. A Bruker X-ray generator with graphite monochromatized Cu-Kα radiation was used. The WAXD patterns were collected by a two-dimensional image detector.

RESULTS

SEM

Figure 1 shows the SEM photomicrographs of the PP/EBM1 blends. EBM1 was etched away by heptane. In PPEBM1-80 blend, EBM1 was the dispersed phase. In PPEBM1-20 blend, PP was the dispersed phase with size of around 2.3 μm. The blend sample disappeared completely in hot heptane remaining PP particles in the solvent. In PPEBM1-80 blend,

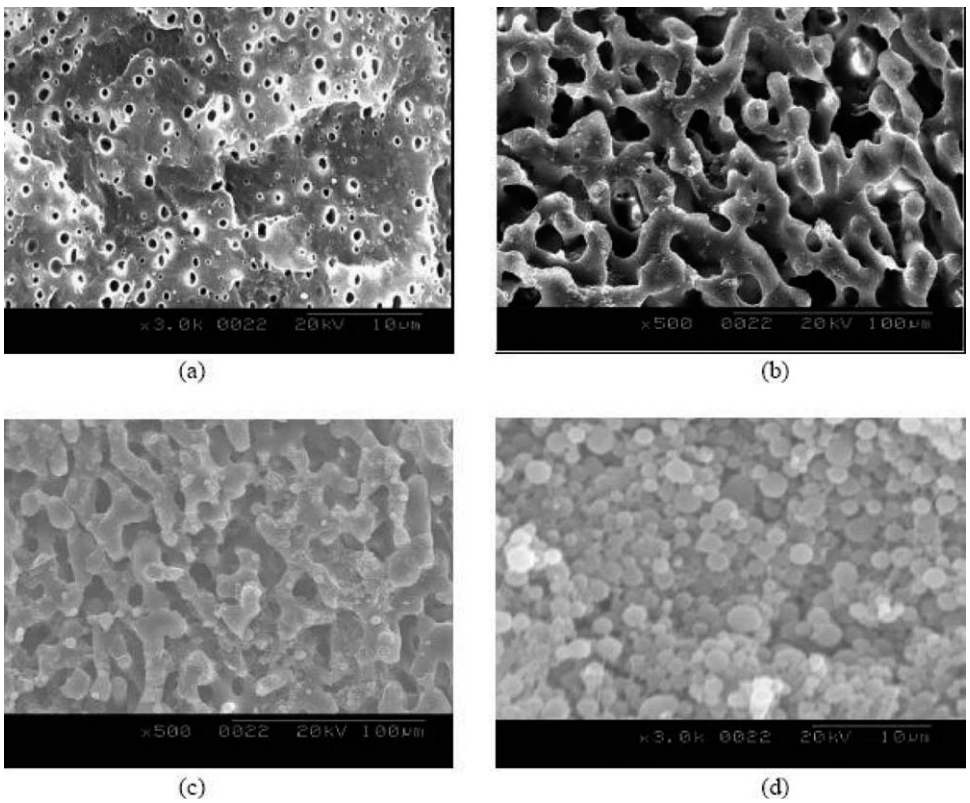

Figure 1 SEM photomicrographs of heptane etched PP/EBM1 blends. (a) PPEBM1-80; (b) PPEBM1-60; (c) PPEBM1-40; (d) PPEBM1-20.

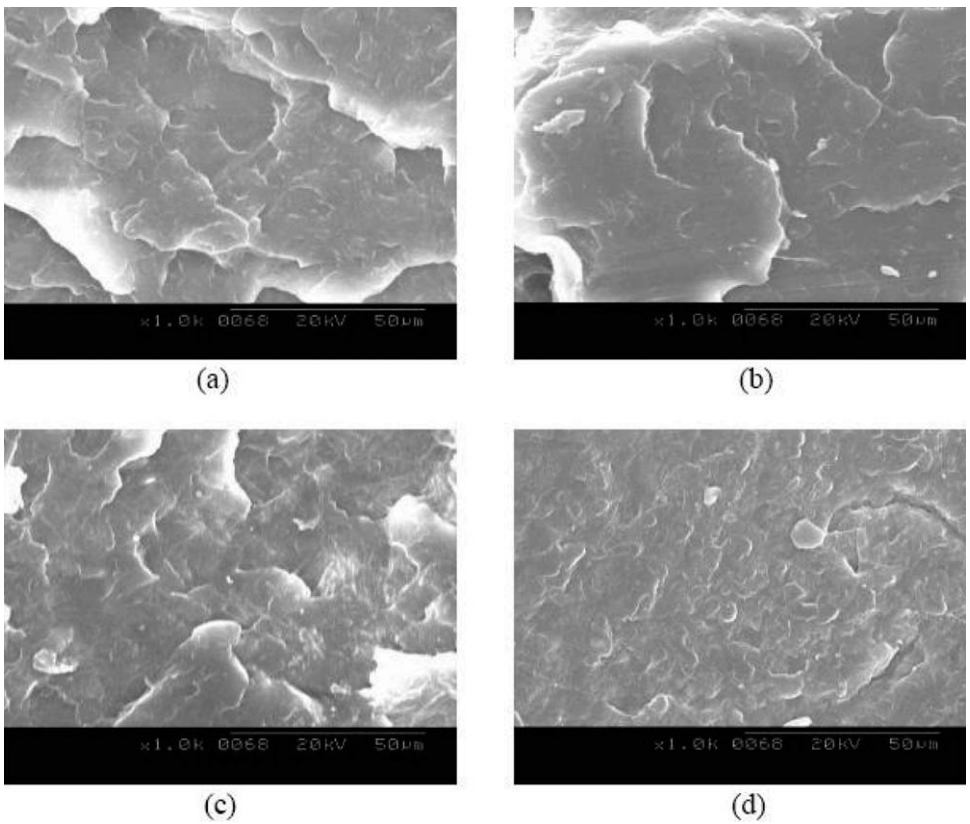

Figure 2 SEM photomicrographs of PP/EBM2 blends[1]: PPEBM2-80; (b) PPEBM2-60; (c) PPEBM2-40; (d) PPEBM2-20.

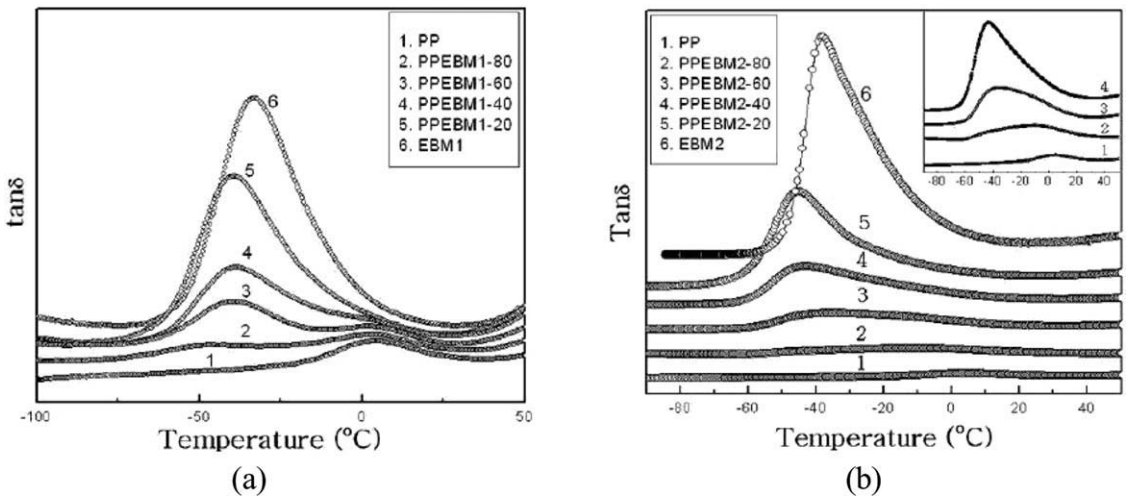

Figure 3 Tan δ versus temperature of (a) PP/EBM1 blends and (b) PP/EBM2 blends in DMA test.

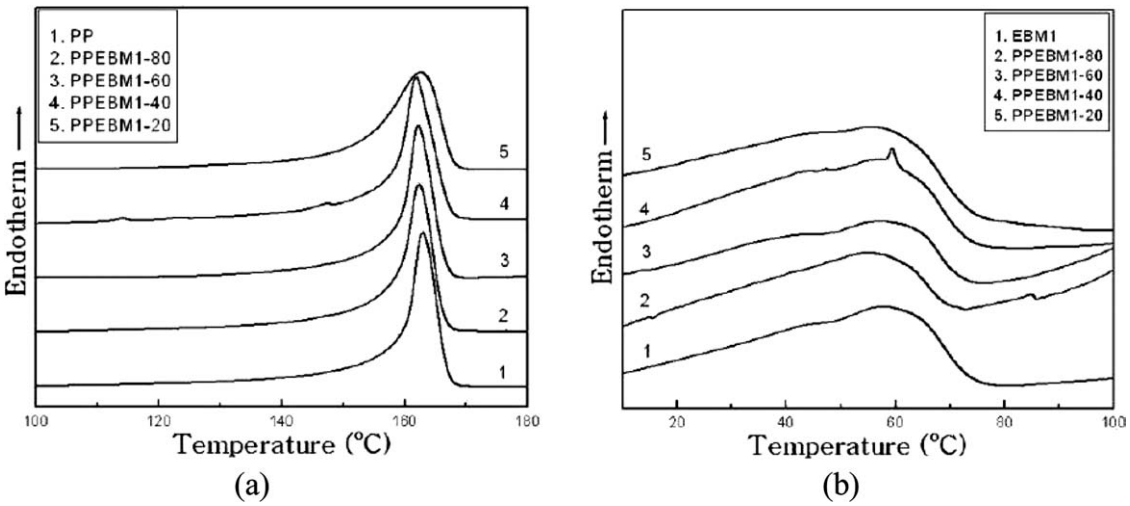

Figure 4 DSC melting curves of PP/EBM1 blends: (a) PP melting peaks; (b) EBM1 melting peaks. Heating rate was 20°C/min.

EBM1 was the dispersed phase. In PPEBM1-40 and PPEBM1-60 blends, co-continuous phases were formed.

Figure 2 shows the SEM photomicrographs of the PP/EBM2 blends. After etching, the samples became white color. The PPEBM2-20 sample did not disappear, unlike PPEBM1-20 sample, but just shrank severely. All the samples exhibited homogeneous morphology. There was no two phase morphology as PPEBM1 blends.

DMA

Figure 3 shows the tan δ versus temperature curves of the PP/EBM1 blends. All the blends had two tan δ peaks which related to the glass transition of the PP and EBM1, respectively. Figure 4 shows the tan δ versus temperature curves of the PP/EBM2 blends. EBM2 exhibited a glass transition temperature (T_g)

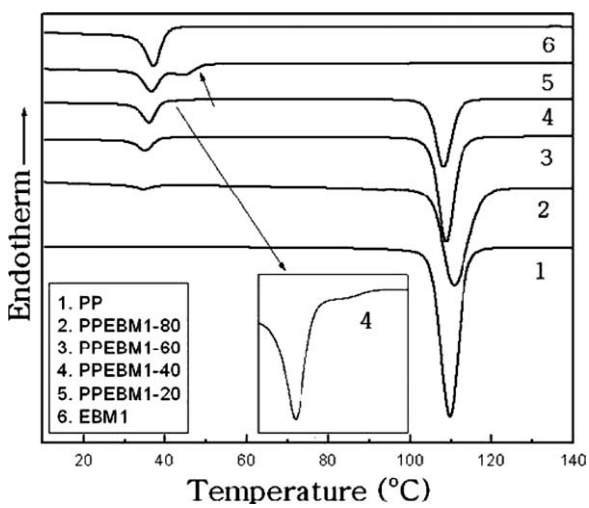

Figure 5 DSC crystallization curves of PP/EBM1 blends. The cooling rate was 20°C/min.

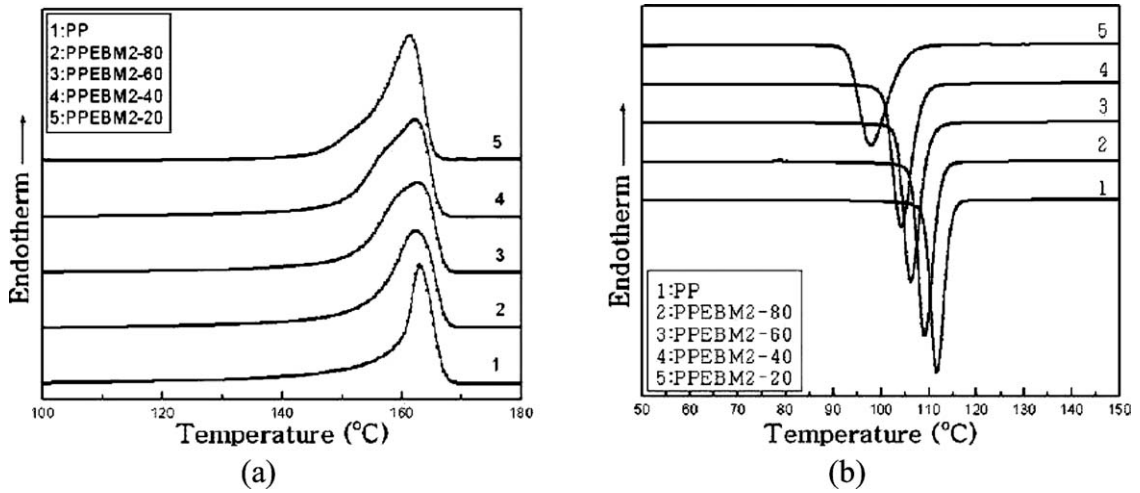

Figure 6 DSC curves of PP/EBM2 blends. Heating and cooling rates were 20°C/min. (a) PP melting peaks; (b) PP crystallization peaks.

at around −39°C and PP exhibited a T_g at around 5°C. With EBM2 content increasing, the T_g of the PP/EBM2 blends decreased. Pure EBM2 showed a higher T_g than PPEBM2-20. All the blends showed only one tan δ peak.

Nonthermal crystallization

Figures 4 and 5 show the DSC melting and crystallization curves of the PP/EBM1 blends. Both PP and EBM1 had hardly any effect on the melting behavior of each other. PP crystallized at around 110°C in PPEBM1-80, PPEBM1-60, and PPEBM1-40 blends as in neat PP. In the PPEBM1-20 blend, PP crystallized at a much lower temperature, around 45°C. There was a peak shoulder at high temperature side of the EBM1 crystallization peak of the PPEBM1-40 blend.

Figure 6 shows the DSC curves of the PP/EBM2 blends. EBM2 could slightly decrease the melting temperatures of the PP and broaden the melting peaks. At blends with 60 and 80 wt % of EBM2, a new melting peak occurs at low temperature side. EBM2 could obviously decrease the crystallization temperatures of the PP. Figure 7 shows the PP content versus crystallization temperatures of the PP/EBM1 and PP/EBM2 blends. EBM1 had hardly any effect on the PP crystallization temperatures at PP contents above 40 wt %. However, below 20 wt % of PP contents, EBM1 could largely decrease the PP crystallization temperatures from around 110–45°C.

Figures 8–11 show the effect of cooling rates on the crystallization and melting behavior of the PP phase in PP, PPEBM1-20 and PPEBM2-20 blends. As shown in Figure 11, with increasing cooling rates, the PP crystallization peaks gradually decreased in all the samples. Figure 9 shows that at cooling rates of 20 and 40°C/min, the PP phase in PPEBM1-20 blend only showed one crystallization peak near the EBM1 crystallization peak. At lower cooling rates, the PP phase showed another crystallization peak at higher temperatures. Figure 10 shows that at cooling rates below 20°C/min the PP phase showed double melting peaks in the PPEBM2-20 blend but not in the pure PP and PPEBM1-20 blend.

Iso-thermal crystallization

Figures 12–14 show the isothermal crystallization dynamics of the PP phase in PP/EBM1 and PP/EBM2 blends. PP phase in all the blends shows the similar nucleation parameter. The PP phase crystallization

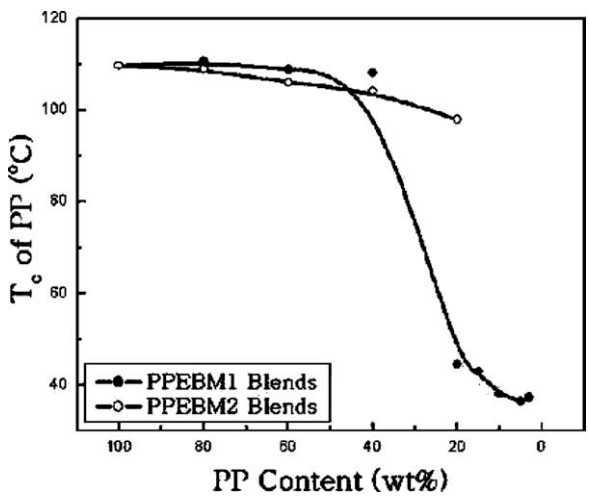

Figure 7 Effect of PP content in PP/EBM1 and PP/EBM2 blends on crystallization temperatures of PP. DSC scanning rate was 20°C/min.

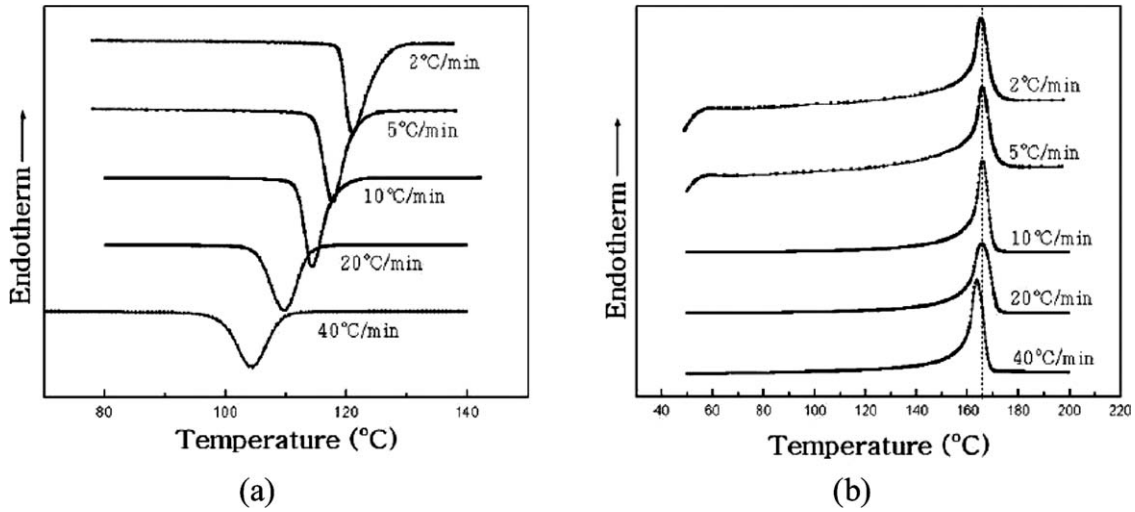

Figure 8 Effect of cooling rates (shown in the figures) on DSC curves of PP: (a) PP crystallization peaks; (b) PP melting peaks at heating rate of 20°C/min.

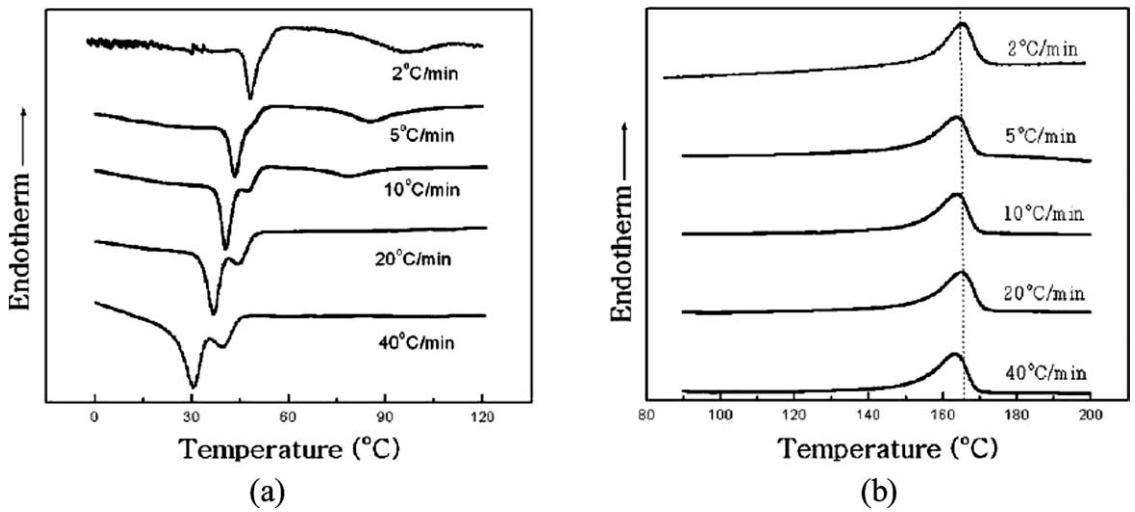

Figure 9 Effect of cooling rates (shown in the figures) on the DSC curves of PPEBM1-20 blend: (a) PP crystallization peaks; (b) PP melting peaks at heating rate of 20°C/min.

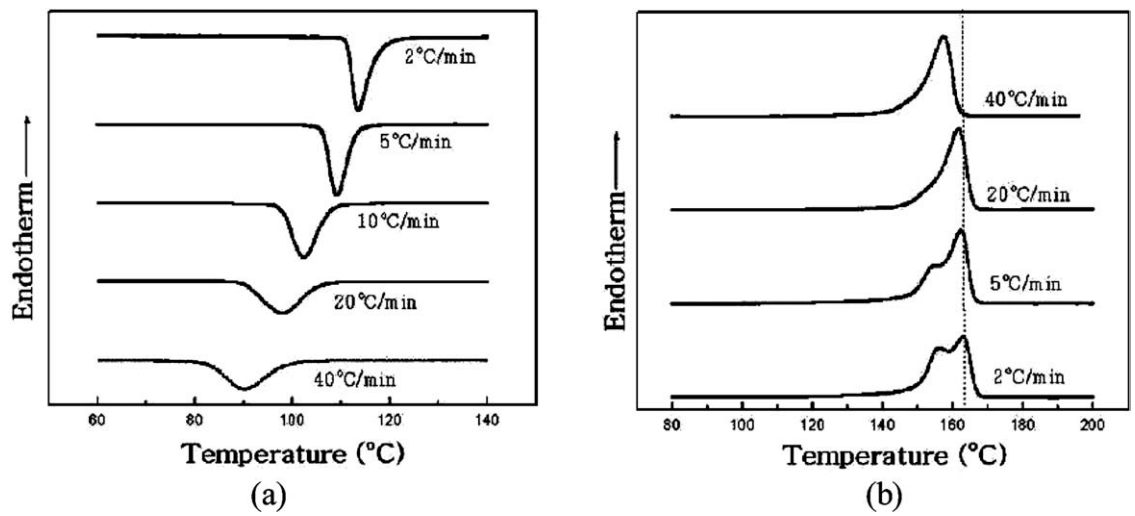

Figure 10 Effect of cooling rates (shown in the figures) on DSC curves of PPEBM2-20 blend: (a) PP crystallization peaks; (b) PP melting peaks at heating rate of 20°C/min.

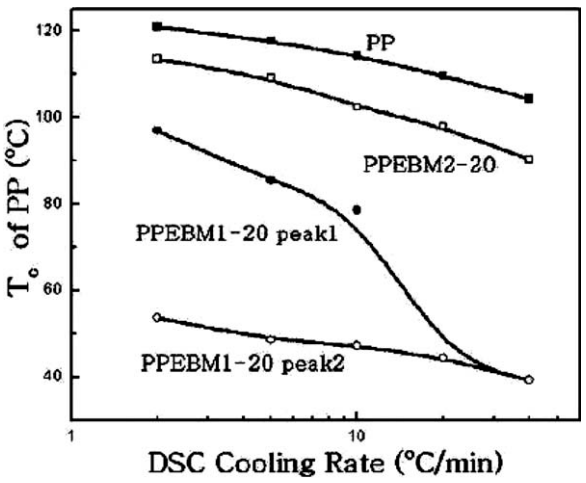

Figure 11 Effect of cooling rates on crystallization temperatures of PP phase in PP, PPEBM1-20, and PPEBM2-20 blends.

rate constants decreased gradually with increasing EBM2 phase. Adding 20 wt % of EBM1 could slightly increase the PP crystallization rate constant. It then decreased slightly with increasing EBM1 phase up to 60 wt %. When EBM1 content was 80 wt %, the PP phase crystallization rate constant decreased sharply.

WAXD

Figure 15 shows the WAXD patterns of the PP, PP/EBM1, and PP/EBM2 blend fibers melt spun at DDR of around 1200. The diffraction arcs were from the PP molecule orientation. The PP presented α-form monoclinic crystal structure determined by Natta and Corradini.[36] The four diffraction planes from inside to outside of the pattern were (110), (040), (130), and (111) Adding EBM1 and EBM2 did not change its crystal type. Plane (110) exhibited a bi-model orientation. One group of planes oriented perpendicular to the fiber direction and the other group of planes oriented along the fiber direction by around 10°. This is related to the unique epitaxial lamellar crystallization behavior of isotactic PP.[16,22] On a parent lamella, secondary daughter lamellae grow epitaxially by sharing the same crystallographic b-axis. Parent and daughter lamellae meet at an angle of about 100°.

The X-ray diffraction intensity of both daughter plane (110) and parent plane (110) were integrated. The integrated diffraction intensity ratio between daughter plane (110) and parent plane (110) was calculated based on eq. (2) as

$$\delta = \frac{\int_0^{\theta_1} I \sin\theta d\theta}{\int_{\theta_1}^{\pi/2} I \sin\theta d\theta} \quad (2)$$

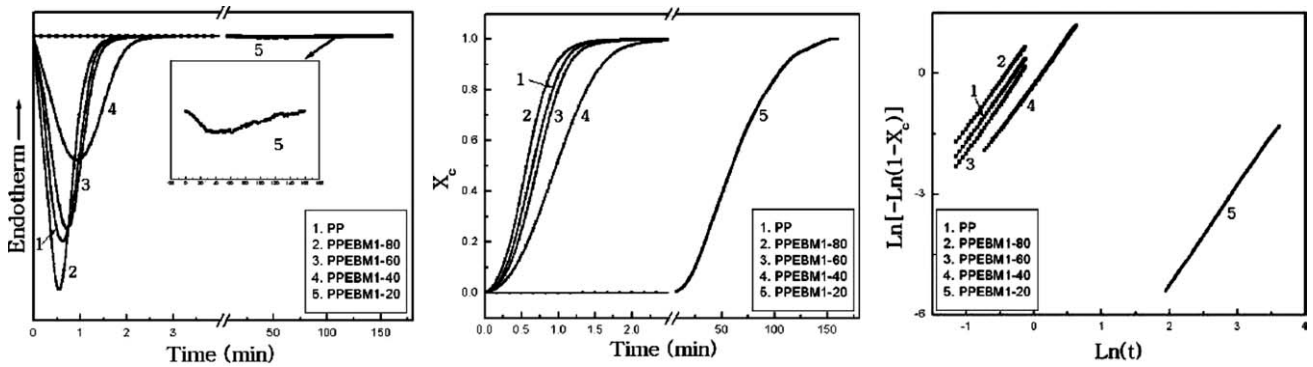

Figure 12 Isothermal crystallization kinetics of PP in PP/EBM1 blends at 120°C.

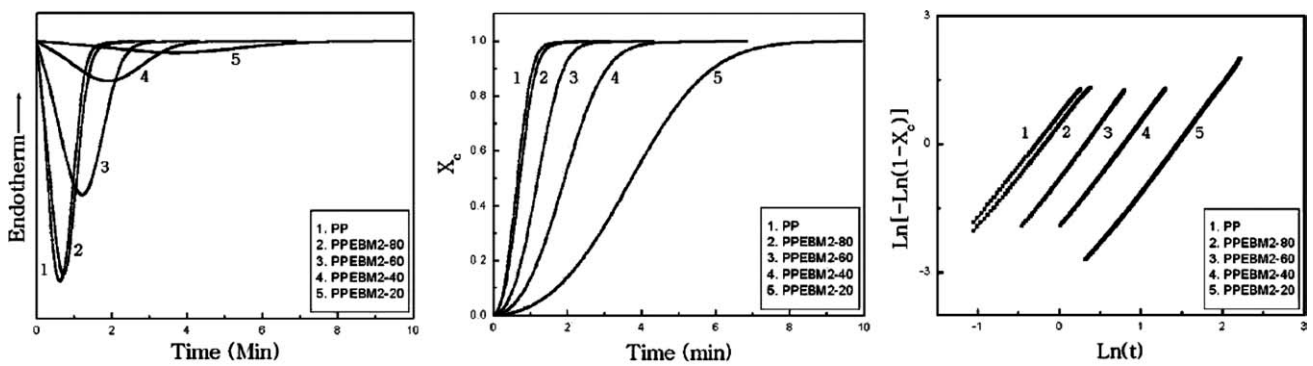

Figure 13 Isothermal crystallization kinetics of PP in PP/EBM2 blends at 120°C.

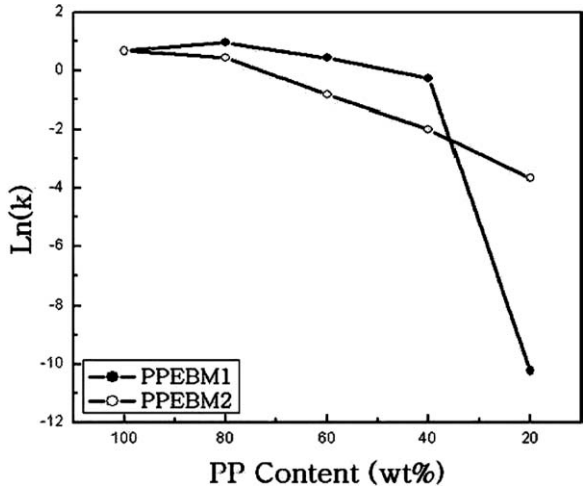

Figure 14 Effect of PP content on the Avrami isothermal crystallization rate constant of the PP phase in PP/EBM1 and PP/EBM2 blends at 120°C.

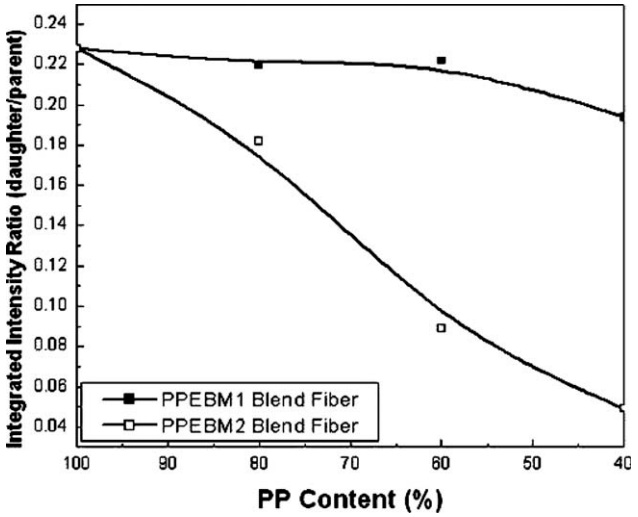

Figure 16 Effect of PP content on the integrated X-ray intensity ratio between daughter lamellae (110) plane and parent lamellae (110) plane from PP, PP/EBM1, and PP/EBM2 blend fibers spun at DDR around 1200. All intensity ratios were divided by the diffraction ratio of the PP fibers.

where θ is the angle between the fiber and plane, (110) I is the diffraction intensity at θ angle, and θ_1 is the angle at which the lowest diffraction intensity occurred. Figure 16 shows that adding EBM1 only slightly affects the diffraction intensity ratio of the daughter plane (110) to the parent plane (110) of the PP phase, which was round 0.22, while adding EBM2 could largely decrease the diffraction intensity ratio.

DISCUSSION

The results of SEM (Figs. 1 and 2) and DMA (Fig. 3) supported that the PP was immiscible with EBM1 and miscible with EBM2. This is consistent with the results published by Yamaguchi et al.[31–33]

Figure 4 presents that both the PP and EBM1 had little effect on the melting peaks of each other. Because they were immiscible, both their melting and crystallization would occur independently. The PP also did not exhibit the nucleation effect on EBM1. However, when the PP was dispersed in the EBM1 matrix (in PPEBM1-20 blend), its crystallization temperature decreased from around 110°C to around 45°C. This is called a fractionated crystallization behavior. It is generally thought that the crystallization of PP at around 110°C is nucleated by heterogeneous nuclei. When PP is dispersed in EBM as small droplets, only very small portion of PP droplets have the heterogeneous nuclei. Thus, most of the PP droplets cannot crystallize at around 110°C. Instead they crystallize at much lower temperature where homogeneous crystallization happens. PPEBM1-40 blend also showed a small shoulder at high temperature side of the EBM1 crystallization peak. This was from the part of the dispersed PP phase in the EBM1 matrix as shown in Figure 1(c). Though the PP phase in the PPEBM1-20 blend crystallized at much lower temperature, it exhibited similar melting temperature as pure PP except a broader melting peak.

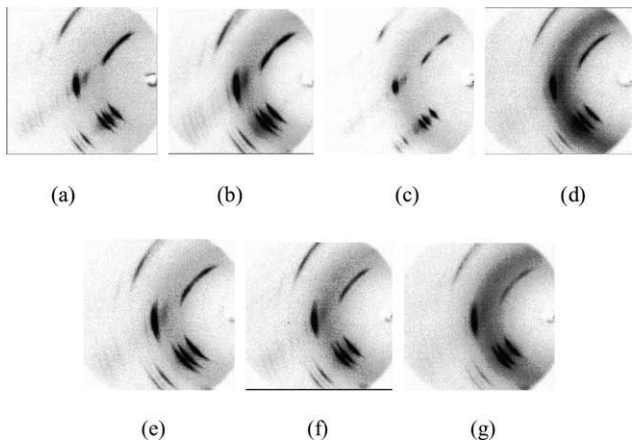

Figure 15 WAXD patterns of (a) PP; (b) PPEBM1-80; (c) PPEBM1-60; (d) PPEBM1-40; (e) PPEBM2-80; (f) PPEBM2-60; (g) PPEBM2-40 fibers melt spun at DDR around 1200.

Figure 6 shows that EBM2 could obviously decrease the crystallization temperatures of the PP phase. EBM2 was miscible with the PP. Thus it diluted the PP molecule concentration. This may decrease both the nucleation rate and the crystallization growth rate. Yamaguchi et al. reported[32] that one miscible EBM could decrease the PP spherulite growth rate, while one immiscible EBM did not affect the PP spherulite growth rate. Their results were consistent with the study in this manuscript. EBM2 slightly decreased the melting temperature of the PP phase and broadened the PP melting peaks

obviously. When EBM2 content was above 40 wt %, the PP melting peak seemed to become double melting peaks. Figures 8 and 9 show that cooling rate had little effect on the PP melting behavior in both pure PP and PPEBM1-20 blend. At the cooling rate of 40°C/min, the polypropylene was quenched and showed slightly decreased melting temperatures.

Figure 10 shows that obvious double melting peaks formed in PPEBM2-20 blend at cooling rates of 5°C/min and 2°C/min. These double melting peaks might form the PP epiaxial crystal lamellae. As we mentioned in the Introduction, the isothermal crystallization temperatures of the iPP could be divided into four groups. When iPP crystallized at group I (below 122°C), it formed very small spherulite and cross-hatched lamellae with the same thickness at both radial and tangential direction. The sample showed one melting peak at high DSC scanning rate and double melting peaks with low DSC scanning rate because the recrystallization could happen. When iPP crystallized at group II (from 122 to 135°C), it still formed cross-hatched lamellae with the same thickness. It exhibited only one melting peak and recrystallization phenomena did not happen. When iPP crystallized at group III (from 135 to 152°C), it formed larger spherulites. Cross-hatched lamellae formed the spherulite core. At outside layer of the spherulite, radial lamellae showed thicker thickness than the tangential lamellae. Thus the sample exhibited double melting peaks. When iPP crystallized at group IV (above 152°C), it formed very large spherulites. The thicker radial lamellae dominated the spherulites. Thus the sample only showed one melting peak. Adding EBM2 into iPP could largely decrease the nucleation rate, thus the iPP could form bigger spherulites with the similar structure as the spherulites formed in group III. Thus it demonstrated double melting peaks. Both Yamaguchi et al.[32] and Thomman et al.[34] presented that miscible EBM could largely increase the iPP spherulite sizes.

Figure 9 shows that when PPEBM1-20 was crystallized at 10°C/min, 5°C/min, and 2°C/min, the PP exhibited another crystallization peak at higher temperatures except the one at around 45°C. One possible reason is that the longer annealing time at slower cooling rates increased the PP droplets coalescence, which increased the portion of PP with nuclei. More studies should be done to fully understand this phenomenon.

Figure 14 shows that adding EBM2 could largely decrease the crystal growth rate constant of the PP phase. As we mentioned above, this was because of the dilute effect of the EBM2 to the PP molecules. Adding EBM1 also could slightly decrease the crystal growth rate constant when the PP was continuous phase. This was because the EBM1 phase could physically block the iPP spherulite growth path. When the PP phase became dispersed phase in PPEBM1-20 blend, the fractionated crystallization largely decreased its crystal growth rate constant.

Figure 15 shows that both EBM1 and EBM2 did not change the crystal type of the PP. It was very interesting that EBM2 could largely decrease the daughter plane (110) as shown in Figure 16. Figure 15(g) also shows that the daughter plane (110) had much lower intensity comparing with the parent plane (110) in the PPEBM2-40 fiber. In the iPP crystallization, the EBM2 molecules were gradually excluded into between the radial lamellae. This largely diluted the PP molecule concentration between these radial lamellae. This may largely retard the epiaxial crystallization. However, more detailed study should be done about this phenomenon.

CONCLUSIONS

The crystallization behavior of the iPP in its EBM blends was strongly dependent on its miscibility with the EBMs. EBM1 had 12.5 mol % of butene and was immiscible with the PP. It had little effect on both the crystallization and melting behavior of the continuous PP phase. But when the PP was dispersed in the EBM1, its crystallization rates were largely decreased because of the fractionated crystallization behavior. EBM2 had 57.5 mol % of butene and was miscible with the PP. It could largely decrease the crystallization rates of the PP phase because the EBM2 molecules diluted the PP molecule concentration, and thus decreased both the nucleation and crystallization growth rates.

At slow cooling rates, the PP showed double melting peaks in PPEBM2-20 blend but not in its pure state and PPEBM1-20 blend. EBM2 might increase the PP spherulite sizes which might include both thicker radial parent lamellae and thinner tangential daughter lamellae. The EBM2 also could largely decrease the daughter (110) plane amount of the PP phase. When EBM2 molecules were excluded out and stayed between the PP lamellae, it largely diluted the PP molecules. This might suppress the growth of the daughter lamellae.

We thank Dr. Masayuki Yamaguchi of Tosoh, Corp., now with Japan Advanced Institute of Science and Technology for providing us ethylene butene copolymer with 57.4 mol % of butene and provided its molecular weights. We thank Dr. Sunny Jacob in Exxon Mobil Chemical who provided us ethylene–butene copolymer with 12.5 mol % of butene and provided its molecular weights.

References

1. Montecatini, Ital. Pat. 1954, 535, 712; 535, 425.
2. Montecatini, Ital. Pat. 1954, 526, 101.
3. Padden, F. J.; Keith, H. D. J Appl Phys 1959, 30, 1479.

4. Cox, W. W. Polym Eng Sci 1967, 7, 309.
5. Petraccone, V.; Guerra, G.; De Rosa, C.; Tuzi, A. Macromolecules 1985, 18, 814.
6. Yadav, Y. S.; Jain P. C. Polymer 1986, 27, 721.
7. Monasse, B.; Haudin, J. M. Colloid Polym Sci 1985, 263, 822.
8. Maiti, P.; Hikosaka, M.; Yamada, K.; Toda, A.; Gu, F. M. Macromolecules 2000, 33, 9069.
9. Yamada, K.; Hikosada, M.; Toda, A.; Yamazaki, S.; Tagashira, K. Macromolecules 2003, 36, 4790; 4802.
10. Naiki, M.; Kikkawa, T.; Endo, Y.; Nozaki, K.; Yamamoto, T.; Hara, T. Polymer 2000, 42, 5471.
11. Kim, Y. C.; Ahn, W.; Kim, C. Y. Polym Eng Sci 1997, 37, 1003.
12. Petraccone, V.; De Rosa, C.; Guerra, G.; Tuzi, A. Makromol Chem Rapid Commun 1984, 5, 631.
13. Alamo, R. G.; Brown, G. M.; Mandelkern, L.; Lehtinen, A.; Paukkeri, R. Polymer 1999, 40, 3933.
14. Sauer, J. A.; Morrow, D. R.; Richardson, G. C. J Appl Phys 1965, 36, 3017.
15. Khoury, F. J Res Nat Bur Stand A 1966, 70, 29.
16. Binsbergen, F. L.; De Lange, B. G. M. Polymer 1968, 9, 23.
17. Norton, D. R.; Keller, A. Polymer 1985, 26, 704.
18. Olley, R. H.; Bassett, D. C. Polymer 1989, 30, 399.
19. Weng, J.; Olley, R. H.; Bassett, D. C.; Jaaskelainen, P. J Macromol Sci B41, 891 2002.
20. Weng, J.; Olley, R. H.; Bassett, D. C.; Jaaskelainen, P. J Polym Sci Part B Polym Phys 2003, 41, 2342.
21. Janimak, J. J.; Cheng, S. Z. D.; Giusti, P. A.; Hsieh, E. T. Macromolecules 1991, 24, 2253.
22. Lotz, B.; Wittmann, J. C. J Polym Sci Polym Phys 1986, 24, 1541.
23. Ghijsels, A.; Groesbeek, N.; Yip, C. W. Polymer 1982, 23 1913.
24. Holsti-Miettinen, R.; Seppälä, O. T.; Ikkala, O. T. Polym Eng Sci 1992, 32, 868.
25. Manaure, A. C.; Morales, R. A.; Sánchez, J. J.; Müller A. J. J Appl Polym Sci 1997, 66, 2481.
26. Santana, O. O.; Muller, A. J Polym Bull 1994, 32, 471.
27. Vonnegut, B. J Colloid Sci 1948, 3, 563.
28. Cormia, R. L.; Price, F. P.; Turnbull, D. J Chem Phys 1962, 37, 1333.
29. Wunderlich, B. Macromolecular Physics; Academic Press: New York, 1976; vol. 2, p. 36.
30. Groeninckx, G.; Vanneste, M.; Everaert, V. In Polymer Blends Handbook; Utracki, L. A., Ed.; Kluwer Academic: Boston, 2002; Vol. 1, p. 260.
31. Yamaguchi, M.; Miyata, H.; Nitta, K. J Appl Polym Sci 1996, 62, 87.
32. Yamaguchi, M.; Miyata, H.; Nitta K. J Polym Sci Polym Phys 1997, 35, 953.
33. Yamaguchi, M.; Miyata, H. Macromolecules 1999, 32, 5911.
34. Thomann, Y.; Suhm, J.; Thomann, R.; Bar, G.; Maier, R. D.; Mulhaupt, R. Macromolecules 1998, 31, 5441.
35. Avarami, M. J Chem Phys 1939, 7, 1103.
36. Natta, G.; Corradini, P. J Polym Sci 1959, 39, 29.